Earthq Eng & Eng Vib (2015) 14: 517-526 **DOI**:10.1007/s11803-015-0041-2

Seismic stability assessment of an arch dam-foundation system

Pan Jianwen†, Xu Yanjie‡, Jin Feng§ and Wang Jinting§

State Key Laboratory of Hydroscience and Engineering, Tsinghua University, Beijing 100084, China

Abstract: A seismic stability assessment of arch dam-foundation systems is presented using a comprehensive approach, in which the main factors that significantly influence the seismic response of an arch dam-foundation system are considered. A large scale finite element model with over 1 million degrees of freedom is constructed for the Baihetan arch dam (289 m high), which is under construction in the Southwest of China. In particular, the complicated geological conditions with faults intersecting interlayer shear weakness zones at the dam base and the dam abutment resisting force body is modeled in the analysis. Three performance indices are adopted to assess the seismic stability of the arch dam. The results demonstrate that the opening of the joints of the Baihetan arch dam is small and the water stop installed between the joints would not be torn during a design earthquake. The yielding formed in the interface between the dam and foundation does not reach the grouting curtain that would remain in an elastic state after an earthquake. The yielding zones occurring on the upper portion of the dam faces extend 1/8 thickness of block section into the dam body and thus cantilever blocks need not be concerned with sliding stability. The faults and interlayer shear weakness zones in the near field foundation exhibit severe yielding, and a potential sliding surface is penetrated. Although the factor of safety against sliding of the surface fluctuates with a decreased trend during an earthquake, the minimum instantaneous value reaches 1.02 and is still larger than 1.0. Therefore, a conclusion is drawn that the Baihetan arch dam-foundation system will remain stable under the design earthquake.

Keywords: arch dam; seismic stability; faults; earthquake

1 Introduction

A number of high arch dams up to 250–300 m in height with huge reservoirs are under construction in southwest China. These high dams are almost all located in seismically active regions where large earthquakes are expected to occur during the operation period of the projects. The geological conditions of the dam sites are complex. There are faults intersecting interlayer shear weakness zones at the dam base and dam abutment resisting force body, which may significantly influence the stability of the dam-foundation system. Failure of a high dam and release of the reservoir may cause loss of numerous human lives and catastrophic consequences in the downstream areas. Therefore, seismic safety evaluation of high arch dam-foundation systems is a crucial issue.

The importance of seismic safety of arch dams has long been recognized, and many studies have been conducted over the past three decades. The earthquake analysis of arch dams is complicated because a three-dimensional model is required to represent the geometry of the dam and the semi-unbounded canyon. In addition, some factors that may significantly influence the dam response must be considered in the earthquake analysis to obtain realistic dynamic behavior of arch dam-foundation systems. These factors include opening of vertical contraction joints, cracking of materials, radiation damping due to infinite foundation and hydrodynamic interaction between the dam and reservoir. Previous research (Fenves *et al*., 1992; Lau *et al*., 1998; Zhang *et al*., 2000) demonstrates that contraction joints may open or slip during intense earthquakes. The joints opening releases arch tensile stresses, and transfers resisting loads from the arches to the cantilevers, resulting in a substantial increase of cantilever stresses. The radiation effect of infinite canyon plays an important role in the earthquake analysis of arch dam-foundation systems. The structural response may be significantly reduced when considering radiation damping compared with neglecting foundation mass and damping (Zhang *et al*., 1988; Zhang *et al*., 2009; Lebon *et al*., 2010; Chopra, 2012; Hariri-Ardebili and Mirzabozorg, 2013). Dam-reservoir interaction is also an important factor affecting the dam response during strong earthquakes. The effect of hydrodynamic pressures at various reservoir operational levels on the seismic behavior of arch dams has been investigated (Hariri-Ardebili *et al*., 2013). In addition, the influence of water compressibility on the earthquake

Correspondence to: Pan Jianwen, State Key Laboratory of Hydroscience and Engineering, Tsinghua University, Beijing 100084, China
Tel: +86-10-6278 6017
E-mail: panjianwen@tsinghua.edu.cn
†Assistant Professor; ‡Associate Professor; §Professor

Supported by: National Natural Science Foundation of China under Grant Nos. 51209120, 51579133 and 51323014, and the Tsinghua University Initiative Scientific Research Program under Grant No. 20131089285

Received March 14, 2014; **Accepted** October 8, 2014

response of an arch dam has been studied (Chopra, 2012; Wang *et al*., 2012). However, the final conclusions concerning the practical significance of the water compressibility effect on dam response is not conclusive (Clough and Ghanaat, 1987). The water compressibility is always neglected in current design and study, and the added mass method is commonly used for arch dam-reservoir interaction because of its simplicity and somewhat conservative nature (Zhang and Jin, 2008). Stresses within a dam body may exceed the material strength when the dam-foundation system is subjected to strong earthquakes, and cracking of dam concrete is expected. Some studies (Valliappan *et al*., 1999; Lotfi and Espandar, 2004; Mirzabozorg and Ghaemian, 2005; Pan *et al*., 2011; Zhong *et al*., 2011) have been conducted to understand the seismic cracking behavior of arch dams, and predict cracking mainly formed in the upper portion of arch dams. The influence of these factors on the dynamic response of arch dams is examined separately. Recently, a comprehensive finite element (FE) approach involving contraction joints opening, radiation damping and cracking of dam concrete has been proposed to more realistically simulate the dynamic behavior of arch dams subjected to intense earthquakes (Pan *et al*., 2009).

The research on seismic safety of arch dams mentioned above assumes foundation rock to be linear elastic. The complicated geological conditions of actual dam sites are simplified and the near-field foundation is treated as homogeneous media, neglecting faults and weakness zones. Cracking of foundation rock and yielding of faults and weakness zones may occur during a strong earthquake. Consideration of nonlinearity of the foundation is necessary in the seismic stability analysis of arch dam-foundation systems.

The nonlinear analysis provides seismic behavior of an arch dam and its performance has been qualitatively identified in earlier studies (Valliappan *et al*., 1999; Lotfi and Espandar, 2004; Mirzabozorg and Ghaemian, 2005; Pan *et al*., 2009; Zhong *et al*., 2011). Zhang *et al*. (2012) have suggested three performance indices for assessment of the seismic safety of arch dams. The performance indices include the following: (i) cracking at dam heel not penetrating the grouting curtain; (ii) cracking of the upper part of the dam body not penetrating the cantilever section; and (iii) maximum contraction joint opening not exceeding an allowable value. Pan *et al*. (2014) have proposed an approximately incremental dynamic analysis associated with the performance indices for seismic performance assessment of arch dams.

In this work, the seismic stability of arch dam-foundation systems is analyzed based on a comprehensive approach (Pan *et al*., 2009). The seismic analysis considers contraction joints opening, radiation damping due to infinite canyon and cracking of dam concrete. In addition, it accounts for yielding of foundation rock and complicated geological conditions with faults intersecting interlayer shear weakness zones in the near-field. A brief description of the comprehensive approach for arch dam-foundation systems is first presented, followed by a case study of the Baihetan arch dam (289 m high) that is under construction in southwest China. A large scale FE model with a total number of degrees of freedom (DOF) of over 1 million is constructed for the dam-foundation system. The seismic stability of the dam-foundation system is then evaluated based on the performance indices suggested by Zhang *et al*. (2012), and conclusions are presented.

2 Arch dam-foundation system modeling

In the comprehensive finite element (FE) approach, the main factors that significantly influence the seismic response of an arch dam-foundation system are considered involving the opening of vertical contraction joints, cracking and yielding of materials (dam concrete and foundation rock with faults), radiation damping due to infinite foundation, and hydrodynamic interaction between the dam and reservoir.

2.1 Elasto-plastic model for concrete and rock

Although several sophisticated nonlinear constitutive models have been developed including, but not limited to, plastic-damage models (Lee and Fenves, 1998) for brittle materials, there is convergence difficulty in large scale numerical simulation of the nonlinear behavior of rock and concrete using these models. The Drucker-Prager elasto-plastic model has good convergence and is widely adopted for simulation of rock and concrete.

The yield surface of the Drucker-Prager model is given as

$$F = \alpha I_1 + \sqrt{J_2} - k \tag{1}$$

where I_1 is the first invariant of stress tensor; J_2 is the second invariant of the deviatoric stress tensor; α and and k are the material parameters.

The Drucker-Prager yield surface in the stress space is a cone that can be considered as a smooth approximation to the Mohr-Coulomb criterion, which is an irregular hexagonal pyramid surface. For the circumcircle matching method (Fig. 1), the conversion relation of material parameters between the two surfaces is obtained:

$$\alpha = \frac{2\sin\phi}{\sqrt{3}(3-\sin\phi)} \tag{2}$$

$$k = \frac{6c\cos\phi}{\sqrt{3}(3-\sin\phi)} \tag{3}$$

where ϕ and c are the friction angle and cohesion, respectively.

The equivalent plastic strain is used as an index to describe cracking (yielding equivalent) of brittle materials. It is defined as

$$\bar{\varepsilon}^{pl} = \int_0^t \dot{\bar{\varepsilon}}^{pl} \mathrm{d}t \tag{4}$$

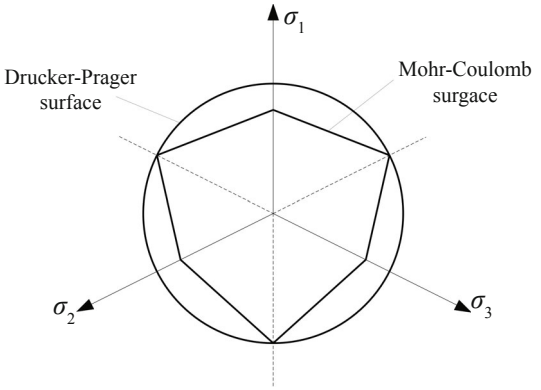

Fig. 1 Drucker-Prager and Mohr-Coulomb criteria in the deviatoric plane

where $\dot{\bar{\varepsilon}}^{pl}$ is the equivalent plastic strain rate. In the previous safety evaluation of arch dams using the Drucker-Prager model (Jin *et al*., 2011), it is a reasonable assumption that cracking of dam concrete and foundation rock is formed due to tension or combined tension-shear loads when the equivalent plastic strain exceeds 100 microstrain.

2.2 Earthquake input method

The radiation damping due to infinite foundation significantly influences the earthquake response of arch dams, and thus, it is required to be considered in the seismic safety evaluation of a dam-foundation system. The viscous-spring artificial boundary (Liu *et al*., 2006) is used to simulate the effect of radiation damping in the FE model, and it demonstrates efficiency and accuracy in seismic analysis of arch dam-foundation systems (Zhang *et al*., 2009). The viscous-spring artificial boundary consists of frequency-independent springs and dampers that are installed on the truncated boundaries of the foundation to closely reproduce the actual response of the far-field rock. The coefficients of the springs and dampers are defined as:

$$K_{li} = a_i \frac{G}{r} \cdot A_l \tag{5}$$

$$C_{li} = b\rho c_i A_l \tag{6}$$

where K_{li} and C_{li} (i = p, s) are, respectively, the spring and damper coefficients associated to node l in the normal direction (i = p) or the tangential direction (i = s) of the truncated boundary; G is the shear modulus; ρ is the mass density of foundation rock; c_i is the P-wave (i = p) velocity or the S-wave (i = s) velocity of the foundation rock; r is the distance from the wave source to the location of node l; A is the tributary area of node l; and a_i and b are the modification parameters.

In the FE model with a viscous-spring artificial boundary, the earthquake cannot be directly input as acceleration time histories in the seismic analysis. The ground motions are converted to equivalent tractions that satisfy the displacement and stress conditions on the truncated boundaries due to the free field in a semi-infinite foundation, and the tractions are exerted on the truncated boundaries (Zhang *et al*., 2009). In this earthquake input method, although the uniform earthquake is input at the foundation base, it may generate spatially varying ground motions at the dam-foundation interface as a result of the wave scattering effect of the canyon.

2.3 Contraction joint model

The vertical contraction joints in arch dams are expected to open and close repeatedly when subjected to strong earthquakes. This nonlinearity significantly influences the dynamic response of the structure in terms of stress distribution and cracking patterns of arch dams. The contraction joints are simulated by means of the contact surface model in this work. The contact surface model consists of a master surface and a slave surface between which the interaction follows the exponential contact pressure-overclosure relation:

$$p = \begin{cases} 0 & \text{for } h \le c \\ \dfrac{p_0}{\mathrm{e}-1}\left(1-\dfrac{h}{c}\right)\left(\mathrm{e}^{1-\frac{h}{c}}-1\right) & \text{for } h > c \end{cases} \tag{7}$$

where p is the contact pressure; h is the overclosure between the contact surfaces; p_0 is a typical pressure value at zero overclosure; and c is the initial contact distance.

Sliding response of contraction joints are governed by Coulomb's friction law. If the shear force $F_s > F_{s,\max} = \mu p$, slip occurs between the contact surfaces of the contraction joints and $F_s = \mu p$ with μ being the friction coefficient.

3 Case study of the Baihetan arch dam

The Baihetan hydropower plant is under construction on the Jinsha River, upstream of the Yangzi River, in southwest China. The installed generation capacity of the plant is 14 GW, with 14 generating units providing 1000 MW each. In terms of generating capacity, it will be the second largest hydropower plant in China, after Three Gorges Dam. The Baihetan project is expected to be complete in 2022. The rendering of the completed project is shown in Fig. 2.

The Baihetan dam is a concrete hyperbolic arch dam

Fig. 2 Rendering of the Baihetan project

with a maximum height of 289 m and an arc length of the crest of 700 m. The thickness at the crest is 13 m, and 72 m at the base. The normal storage level of the reservoir is 825 m and its capacity is 20.6 billion m^3. The dam is located in a seismically active region with Earthquake Intensity VIII. The geological conditions are complex, with several faults intersecting interlayer shear weakness zones at the dam base and the dam abutment resisting force body, which may significantly affect the seismic stability of the arch-foundation system.

3.1 FE modeling of the dam-foundation system

Figure 3 shows the three-dimensional (3D) FE model constructed for the Baihetan arch dam-foundation system. The mesh of the model is created with the use of the 8-node brick element. The 3D FE model of the dam-foundation system is composed of 391314 elements and 349114 nodes with a total number of DOFs over 1 million. The mesh size of the arch dam is about 5 × 5 m^2 in the vertical and tangential directions. Sixteen layers of elements across the dam thickness are used to consider cracks propagating through the dam cantilever blocks. The simulated domain of the foundation is cut from the canyon with H extension in the upstream, left-bank, right-bank and depth directions and 2.5H in the downstream direction, where H is the dam height. The mesh size of the near-field foundation is about 10 m, and 40 m in the far-field foundation. The Baihetan arch dam is built as independent cantilever monoliths separated by 28 vertical contraction joints. A previous study (Zhang *et al*., 2000) demonstrates that the number of contraction joints that needed to be simulated can be reduced and the stress distribution of the dam can be obtained with satisfied accuracy. In this study, 19 contraction joints (denoted by Jn, n = 1, 2, ..., 19) are simulated to conserve computational costs. The dam blocks separated by the contraction joints are then denoted by Bn, n = 1, 2, ..., 20, sorted from the left to right abutment (Fig. 3(c)).

Rock classification is considered in the FE model according to the geological conditions. The faults f222, F18, F14, F16 and F17 and the interlayer shear weakness zones C3, C3-1, C4, LS331, LS3318 and LS337 in the near field foundation are exactly simulated using refined mesh. The element size in the normal direction of the faults is assigned as 1 m. Their distribution is shown in Fig. 4(a) and (b). The intersections of the fault F17 and the interlayer shear weakness zones LS331 and LS3318 form two potential sliding surfaces in the left abutment of the foundation (Fig. 4(c)). The seismic safety against

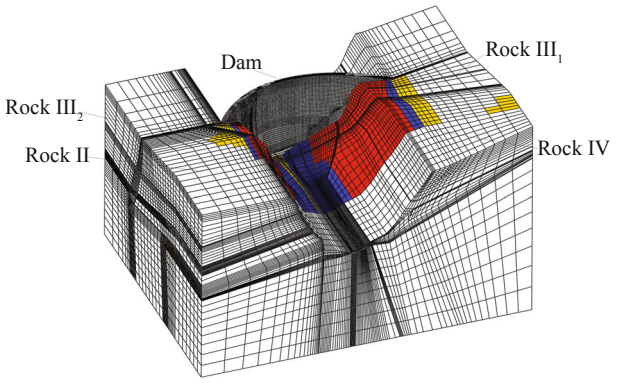

(a) Dam-foundation system

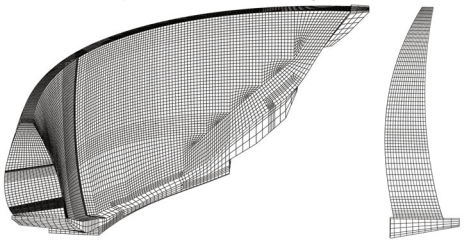

(b) Dam body

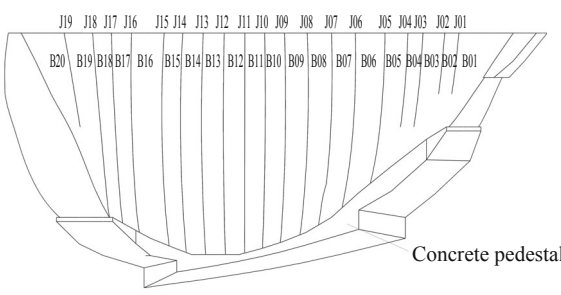

(c) Contraction joints simulated in the model

Fig. 3 FE discretization of the arch dam-foundation system

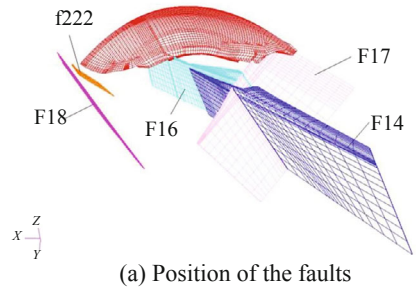

(a) Position of the faults

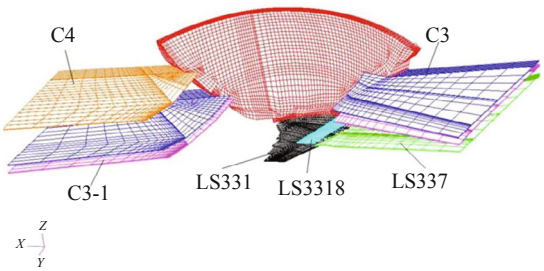

(b) Position of the interlayer shear weakness zones

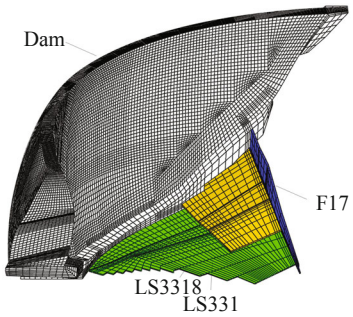

(c) Potential sliding surfaces

Fig. 4 FE mesh for the faults and interlayer shear weakness zones in the near-field foundation

sliding of the potential sliding surfaces is of concern to the dam owner and engineers.

3.2 Material properties and loading conditions

The Drucker-Prager elasto-plastic model is applied to consider material damage and yielding for dam concrete and foundation rocks. The material properties used in the simulation are based on mechanical tests conducted by the dam designer, Huadong Engineering Corporation Limited, and are listed in Table 1 for the dam concrete and foundation rocks, while Table 2 shows the faults and the interlayer shear weakness zones. The interface between the dam and foundation is neglected and its behavior is equivalently modeled according to yielding of concrete and rock with refined elements surrounding the interface.

The gravity stress state of the foundation is set as the initial condition, thus considering the geostress in the simulation. The first applied load is self-weight of the dam with the assumption of independent cantilevers, and then the normal hydrostatic and sediment pressures and the design temperature load. The reservoir water depth is 300.4 m, and the sediment depth is 185.4 m. The buoyant unit weight of sediment is 5.0 kN/m^3 and its frictional angle is assumed to be 0°. The sediment pressure is then treated as hydrostatic pressure and applied on the upstream surface of the arch dam. The earthquake ground motions are then applied to shake the arch dam-foundation system.

The Baihetan arch dam is designed to challenge the design earthquake, whose ground motion has a 2% chance of being exceeded in a 100-year period (or a 5000-year return period). The peak ground acceleration (PGA) of the design earthquake is 0.325 g. The acceleration time histories of the design earthquake are generated using the artificial accelerograms generation method and the components in three directions, i.e. stream, cross-stream and vertical, are shown in Fig. 5. It is expected that damage of the arch dam may be accumulated over time during a strong earthquake. The duration of the earthquake is assumed to be 20 s and the influence of duration on the nonlinear behavior of the structure is not considered.

The structural damping in the dam-foundation system is incorporated using a Rayleigh-type damping and a 5% damping ratio is assumed. The interaction between the dam and reservoir is modeled using the Westergaard's added hydrodynamic mass. The seismic effect of sediment is neglected.

Table 1 Mechanical properties of the dam concrete and foundation rocks

	Dam concrete	Rock II	Rock III_1	Rock III_2	Rock IV
Young's modulus (GPa)	24.00	16.00	10.50	8.00	3.50
Poisson's ratio	0.17	0.22	0.24	0.26	0.31
Frictional coefficient	1.40	1.33	1.15	0.98	0.65
Cohesion strength (MPa)	1.60	1.48	1.10	0.92	0.49

Table 2 Mechanical properties of the faults and interlayer shear weakness zones

	F14	F16	F17	F18	f222	C3	C3-1	C4	LS331	LS3318	LS337
Young's modulus (GPa)	0.32	0.34	0.90	0.72	0.28	0.60	0.16	0.10	2.00	0.02	0.36
Poisson's ratio	0.35	0.35	0.35	0.35	0.35	0.35	0.35	0.35	0.35	0.35	0.35
Frictional coefficient	0.42	0.50	0.35	0.42	0.45	0.41	0.36	0.25	0.65	0.37	0.33
Cohesion strength (MPa)	0.10	0.14	0.04	0.10	0.13	0.10	0.04	0.03	0.15	0.05	0.05

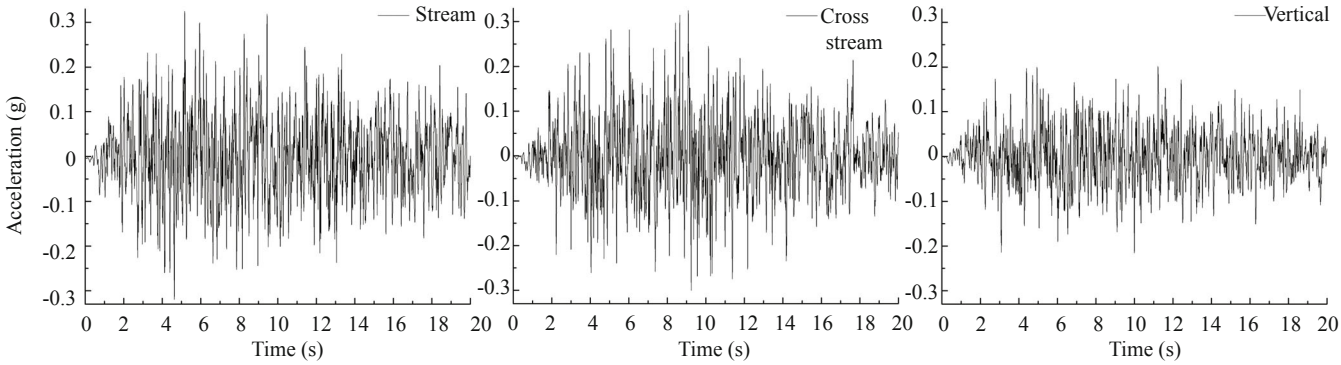

Fig. 5 Input earthquake acceleration histories

3.3 Results and discussion

The seismic analysis of the over 1-million-DOF dam-foundation system takes 165 hours on a computer with dual 6-core Intel(R) Xeon(R) CPU E5-2620 @ 2.00 GHz and 32 GB of system RAM.

The dynamic crest displacements and the opening and sliding of the contraction joints in the Baihetan arch dam are shown in Fig. 6. Larger crest displacements, both in the upstream and downstream directions, occur in the dam blocks located in the middle of the river due to their larger height. The maximum displacements reach about 12 cm in the upstream direction and 14 cm in the downstream direction. It is difficult to directly assess seismic safety of an arch dam in accordance with the dynamic crest displacement. On the contrary, contraction joint opening and sliding can be used as a performance index to evaluate the safety of the copper water stop buried between the adjacent dam blocks. The maximum opening is about 3.2 mm and the maximum sliding is smaller than 40 mm during the design earthquake. The shear keys between the joints are neglected in the simulation, and thus, the sliding of the joints is overestimated and it provides conservative results. An allowance opening of joints, which is approximate 35 mm, is defined to prevent breakage of copper water stop during earthquakes. The calculated joint opening is much smaller than the allowance value and it ensures the seismic safety of the copper water stop.

Cracking of concrete and rock is assumed to form when the equivalent plastic strain exceeds 10^{-4}. Figure 7 shows the evolution of the cracking pattern of the arch dam during an earthquake. Before the earthquake, the dam-foundation system is under static loading conditions and there is no yielding zone in the dam body. Yielding initially occurs on the downstream and upstream faces of dam block B05 near the left abutment at t = 6 s. New yielding zones afterwards occur on the upstream face of dam blocks B07-B09. The yielding on the downstream face propagates along the cross-stream direction and the yielding zone covers dam blocks B04-B08 after the earthquake. The downstream yielding extends towards upstream 1/8 thickness of the dam block section. Partially free cantilevers would not be formed and the seismic sliding stability of the cantilever blocks is warranted. Yielding is also formed on the dam-foundation interface

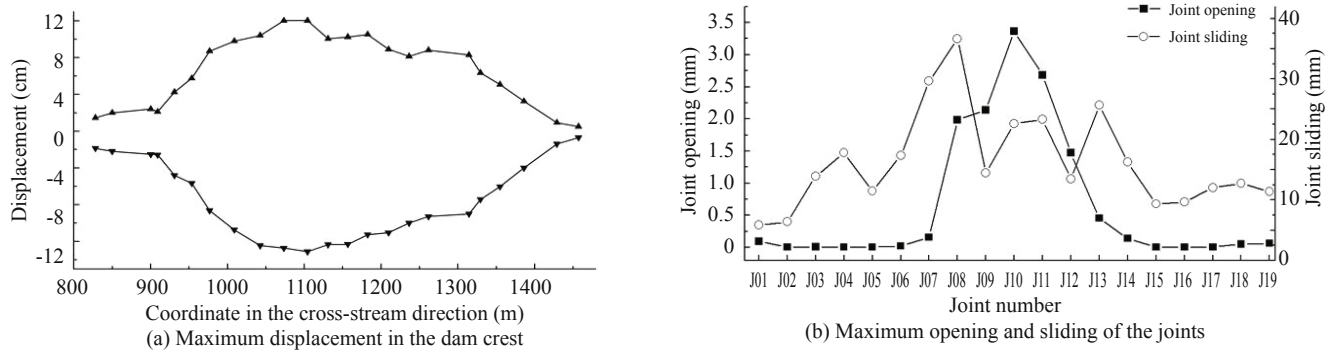

(a) Maximum displacement in the dam crest

(b) Maximum opening and sliding of the joints

Fig. 6 Dynamic response of the arch dam during earthquake

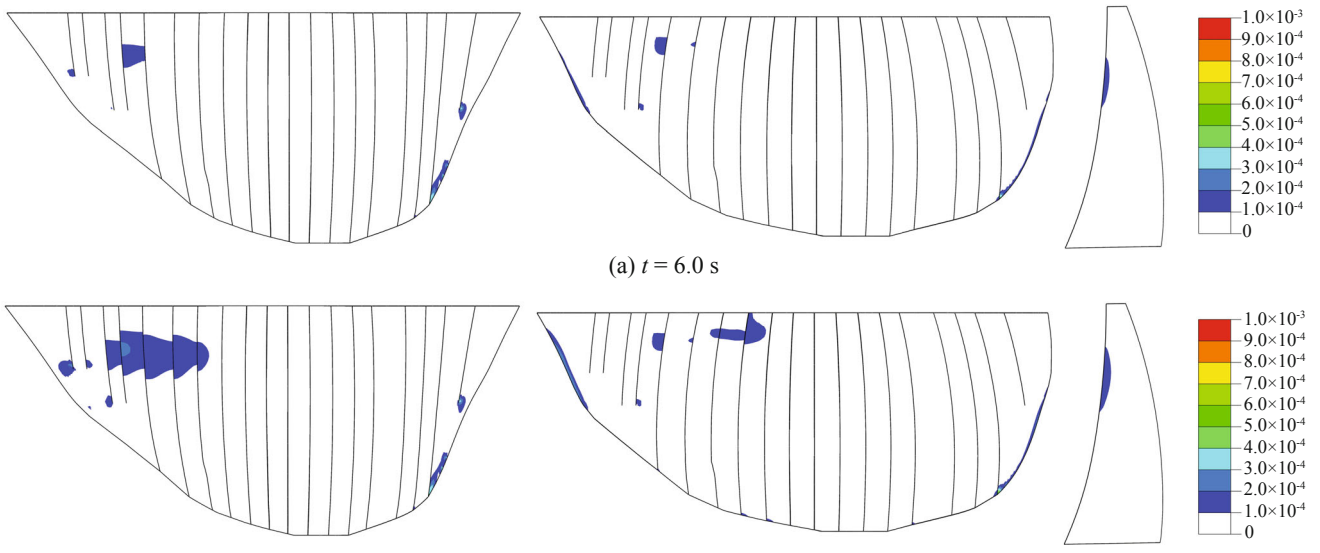

(a) t = 6.0 s

(b) t = 20.0 s

Fig. 7 Yield zones of the dam during earthquake

on both sides of the dam during the earthquake.

The Baihetan arch dam is designed to be located on a concrete pedestal that is installed in the foundation rock. Yielding of the concrete pedestal significantly influences the safety of the grouting curtain. Figure 8 shows the yielding zones of the concrete pedestal. It can be found that minor yielding forms on the interface between the concrete pedestal and the foundation under static loading conditions. After the earthquake, the yielding expands along the interface on the upstream side and extends towards downstream. The yielding does not reach the grouting curtain and the curtain remains in a linear elastic state.

Figure 9 shows a comparison of the yielding zones in the foundation at different elevation profiles before and after the earthquake. It is seen that only fault F18 appears to yield above the elevation of 750 m under static loading conditions. After the earthquake shakes the dam-foundation system, the faults and the interlayer shear weakness zones exhibit severe yielding. In addition, yielding zones form in the left abutment foundation rock between the elevation (EL) of 700 m and 800 m, and an additional yielding zone appears in the right abutment near EL 650 m. These yielding zones in the foundation, especially when forming a sliding surface, may affect the stability of the arch dam-foundation system.

The yielding zones of the potential sliding surfaces F17-LS331 and F17-LS3318 are shown in Fig. 10 and Fig. 11, respectively. There is no yielding on the potential sliding surfaces before the earthquake. The fault F17 suffers severe yielding after the earthquake and the yielding zone is more than half the area of the fault. Only a local yielding zone occurs in the interlayer shear weakness zone LS331, and thus the potential sliding surface F17-LS331 appears not to slide during the design earthquake. Regarding the potential sliding

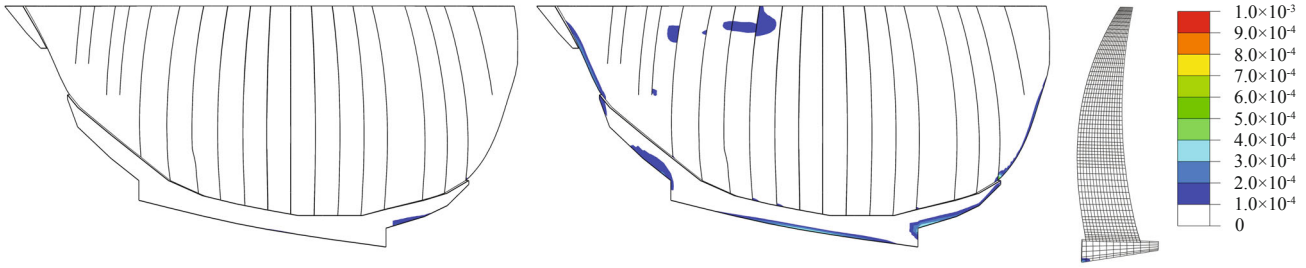

(a) Before earthquake (b) After earthquake

Fig. 8 Yield zones of the concrete pedestal

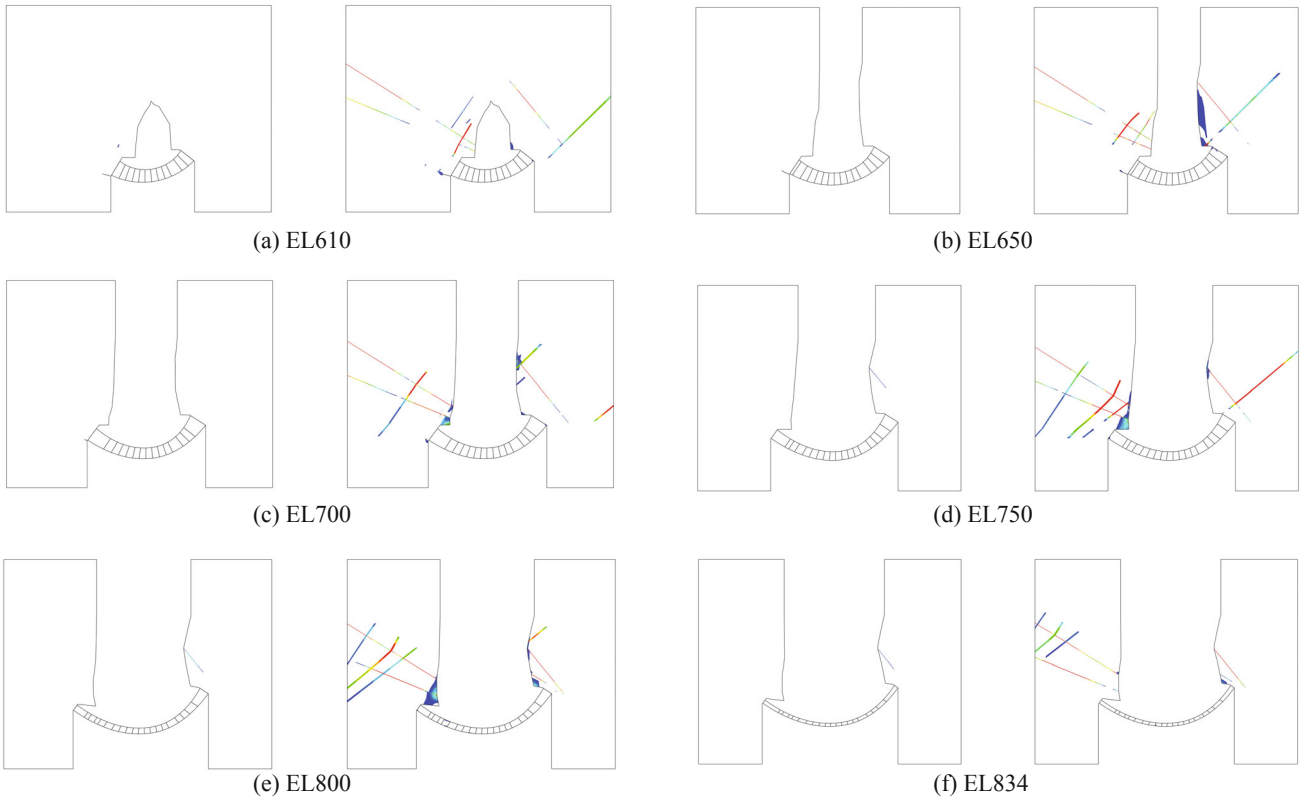

(a) EL610 (b) EL650

(c) EL700 (d) EL750

(e) EL800 (f) EL834

Fig. 9 Yield zones of the foundation at different elevation profiles before and after earthquake

(a) Before earthquake (b) After earthquake

Fig. 10 Yield zones of the potential sliding surface F17-LS331

(a) Before earthquake (b) After earthquake

Fig. 11 Yield zones of the potential sliding surface F17-LS3318

surface F17-LS3318, a large yielding zone forms in the interlayer shear weakness zone LS3318. It is associated with the yielding zone of fault F17, penetrating the potential sliding surface.

A factor of safety against sliding of the potential sliding surfaces is introduced to assess its seismic stability. The factor of safety is defined according to the resistance force F_R and the sliding force F_S; that is $K = F_R / F_S$. The resistance and sliding forces are calculated based on the normal stress σ and the shear stress τ on the sliding surface. The resistance force is written as $F_R = \sum\left(f_j\sigma_j + c_j\right)A_j$ and the sliding force as $F_S = \sum \tau_j A_j$, where j is the node number; A_j denotes the tributary area of node j, and f and c are the frictional coefficient and cohesion strength, respectively. The direction of the sliding force that determines the potentially sliding direction of the surface varies over time during the earthquake.

Figure 12 illustrates the time histories of the sliding safety factor of the two potential sliding surfaces during the earthquake. The trend line is obtained by polynomial fitting of the time history of the sliding safety factor. It can be found that the sliding safety factor of the surface F17-LS331 fluctuates around the value of 2.2 during the earthquake, which is equal to its safety factor under static loading conditions. The minimum safety factor reaches about 1.5, and thus, the potential sliding surface F17-LS331 is stable. The safety factor of the surface F17-LS3318 fluctuates and exhibits a decreased trend during the earthquake. The fluctuating equilibrium value of the safety factor reduces from 1.6 to 1.4 and a minimum instantaneous value of the safety factor reaches 1.02. Thus, the seismic stability of the potential sliding surface F17-LS3318 can be ensured.

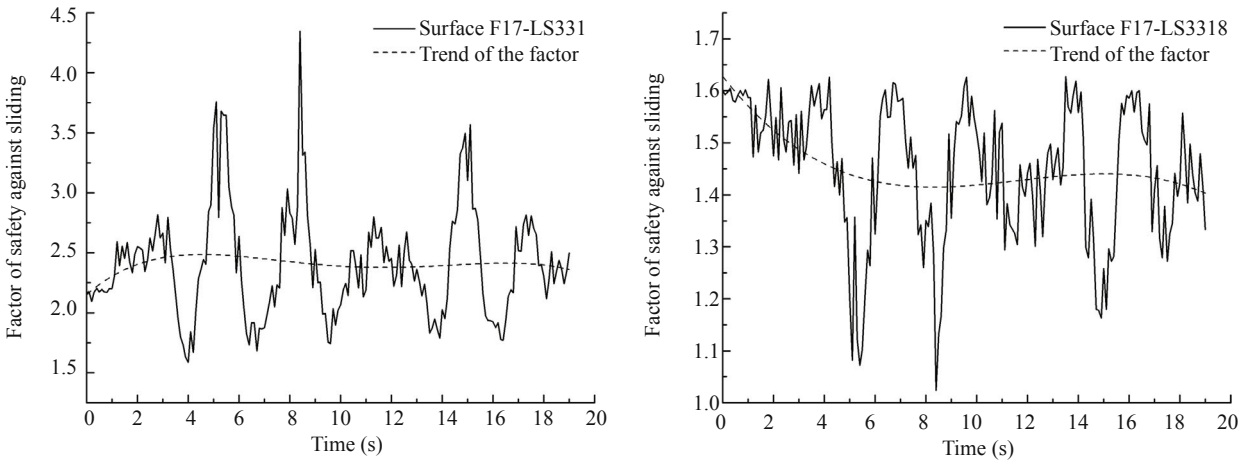

Fig. 12 Factor of safety against sliding of the potential sliding surfaces during earthquake

4 Conclusions

A comprehensive FE model is presented to analyze the seismic stability of arch dam-foundation systems. The simulation considers the main factors that significantly influence the seismic response of the arch dam-foundation system, including opening of contraction joints, nonlinearity of dam concrete and foundation rock, radiation damping and hydrodynamic pressure. The complicated geological conditions with faults intersecting interlayer shear weakness zones at the dam base and the dam abutment resisting force body is modeled. The seismic stability of the dam-foundation system is evaluated based on three performance indices.

The Baihetan arch dam (289 m high), under construction in China, is taken as a case study. A large scale FE model of the Baihetan arch dam-foundation system, in which the total number of DOFs is over 1 million, is constructed. The arch dam-foundation system is designed to withstand an earthquake with peak ground acceleration of 0.35 g. The results from the seismic analysis demonstrate that the maximum opening of the contraction joints during the design earthquake is 3.5 mm, which is much smaller than the allowance opening. Thus, the safety of the copper water stop installed between the joints can be ensured. The yielding in the interface between the dam and the foundation extends from the upstream side towards the downstream direction, and does not reach the grouting curtain which remains in a linear elastic state during the earthquake. Minor yielding appears on the upper portion of the upstream dam face after the earthquake. In addition, a larger yielding zone occurs on the upper portion of the downstream dam face near the left bank abutment. The downstream yielding propagates about 1/8 thickness of the block section into the dam body, and thus, cantilever blocks need not be concerned with sliding stability. The faults and interlayer shear weakness zones in the near field foundation exhibit severe yielding after the earthquake. The yielding penetrates one of the potential sliding surfaces, implying sliding of the rock body above the surface would be possible. The factor of safety against sliding of the potential sliding surface is then used to assess its seismic stability. The time history of the safety factor fluctuates with a decreased trend during the earthquake, and the minimum instantaneous value reaches 1.02, which is still greater than 1.0. Based on the seismic analysis, it can be concluded that the Baihetan arch dam-foundation system will remain stable under the design earthquake.

Acknowledgment

This work was supported by the National Natural Science Foundation of China (Nos. 51209120, 51579133 and 51323014) and the Tsinghua University Initiative Scientific Research Program (No. 20131089285). The authors are grateful for this support. We appreciate Mr. Yao Gui and Mr. Fei Zhu for their contribution to the FE discretization of the model. We also wish to thank the anonymous reviewers for their constructive comments on earlier drafts of this paper.

References

Chopra AK (2012), "Earthquake Analysis of Arch Dams: Factors to Be Considered," *Journal of Structural Engineering*, **138**(2): 205–214.

Clough R and Ghanaat Y (1987), "Experimental Study of Arch Dam-reservoir Interaction," *Proceedings of Joint China-US Workshop on Earthquake Behavior of Arch Dams*, Beijing, China.

Fenves GL, Mojtahedi S and Reimer RB (1992), "Effect of Contraction Joints on Earthquake Response of an Arch Dam," *Journal of Structural Engineering*, ASCE, **118**(4): 1039–1055.

Hariri-Ardebili MA and Mirzabozorg H (2013), "A Comparative Study of Seismic Stability of Coupled Arch Dam-foundation-reservoir Systems Using Infinite Elements and Viscous Boundary Models," *International Journal of Structural Stability and Dynamics*, **13**(06): 1350032.

Hariri-Ardebili M, Mirzabozorg H and Kianoush MR (2013), "Seismic Analysis of High Arch Dams Considering Contraction-peripheral Joints Coupled Effects," *Central European Journal of Engineering*, **3**(3): 549–564.

Jin F, Hu W, Pan J *et al*. (2011), "Comparative Study Procedure for the Safety Evaluation of High Arch Dams," *Computers and Geotechnics*, **38**(3): 306–317.

Lau DT, Noruziaan B and Razaqpur AG (1998), "Modelling of Contraction Joint and Shear Sliding Effects on Earthquake Response of Arch Dams," *Earthquake Engineering and Structural Dynamics*, **27**: 1013–1029.

Lebon G, Saouma V and Uchita Y (2010), "3d Rock-dam Seismic Interaction," *Dam Engineering*, **21**(2): 101.

Lee J and Fenves LG (1998), "Plastic-damage Model for Cyclic Loading of Concrete Structures," *Journal of Engineering Mechanics*, ASCE, **124**(3): 892–900.

Liu J, Du Y, Du X *et al*. (2006), "3D Viscous-spring Artificial Boundary in Time Domain," *Earthquake Engineering and Engineering Vibration*, **5**(1): 93–102.

Lotfi V and Espandar R (2004), "Seismic Analysis of Concrete Arch Dams by Combined Discrete Crack and Non-orthogonal Smeared Crack Technique," *Engineering Structures*, **26**(1): 27–37.

Mirzabozorg H and Ghaemian M (2005), "Non-linear Behavior of Mass Concrete in Three-dimensional Problems Using a Smeared Crack Approach," *Earthquake Engineering & Structural Dynamics*, **34**(3): 247–269.

Pan J, Xu Y and Jin F (2015), "Seismic Performance

Assessment of Arch Dams Using Incremental Nonlinear Dynamic Analysis," *European Journal of Environmental and Civil Engineering*, **19**(3): 305–326.

Pan J, Zhang C, Wang J *et al*. (2009), "Seismic Damage-cracking Analysis of Arch Dams Using Different Earthquake Input Mechanisms," *Science in China Series E-Technological Sciences*, **52**(2): 518–529.

Pan J, Zhang C, Xu Y *et al*. (2011), "A Comparative Study of the Different Procedures for Seismic Cracking Analysis of Concrete Dams," *Soil Dynamics and Earthquake Engineering*, **31**(11): 1594–1606.

Valliappan S, Yazdchi M and Khalili N (1999), "Seismic Analysis of Arch Dams—a Continuum Damage Mechanics Approach," *International Journal For Numerical Methods in Engineering*, **45**(11): 1695–1724.

Wang JT, Zhang CH and Jin F (2012), "Nonlinear Earthquake Analysis of High Arch Dam-water-foundation Rock Systems," *Earthquake Engineering & Structural Dynamics*, **41**(7): 1157–1176.

Zhang CH and Jin F (2008), "Seismic Safety Evaluation of High Concrete Dams Part I: State of the Art Design and Research," *14WCEE*, S13-080, Beijing, China.

Zhang C, Pan J and Wang J (2009), "Influence of Seismic Input Mechanisms and Radiation Damping on Arch Dam Response," *Soil Dynamics And Earthquake Engineering*, **29**(9): 1282–1293.

Zhang C, Wang G and Zhao C (1988), "Seismic Wave Propagation Effects on Arch Dam Response," *9th World Conference on Earthquake Enginnering*, Tokyo-Kyoto, VI: 367–372.

Zhang C, Xu Y, Wang G *et al*. (2000), "Non-linear Seismic Response of Arch Dams with Contraction Joint Opening and Joint Reinforcements," *Earthquake Engineering and Structural Dynamics*, **29**: 1547–1566.

Zhang CH, Xu YJ, Wu MX *et al*. (2012), "The Performance of High Dams in Wenchuan 5-12 Earthquake and Follow-up Analysis of the Shapai Arch Dam during the Event," *15WCEE*, Lisbon, Portugal.

Zhong H, Lin G, Li X *et al*. (2011), "Seismic Failure Modeling of Concrete Dams Considering Heterogeneity of Concrete," *Soil Dynamics and Earthquake Engineering*, **31**(12): 1678–1689.